Supporting Information

Bidirectional ROS cascade amplification in a TME-activatable nanoplatform for MRI-guided sono-chemodynamic cancer therapy

Linrong Shi[1,2], Chenhui He[1], Zhezhu Nan[1], Yang Liu[1], Jiayue Li[1], Mingxi Wan[1], Ping Li[3], and Yi Feng[1]*

[1]The Key Laboratory of Biomedical Information Engineering of Ministry of Education, Department of Biomedical Engineering, School of Life Science and Technology, Xi'an Jiaotong University, Xi'an 710049, China

[2]Department of Diagnostic Radiology, Yong Loo Lin School of Medicine, National University of Singapore, Singapore, 119074, Singapore

[3]MOE Key Laboratory of Thermo-Fluid Science and Engineering, Xi'an Jiaotong University, Xi'an, Shaanxi, 710049, China

*Corresponding Author:

Yi Feng, Email: fengyi@mail.xjtu.edu.cn

Experimental section

Chemicals

Reagents and solvents were used without further purification. Zinc nitrate hexahydrate ($Zn(NO_3)_2 \cdot 6H_2O$, ≥ 99%) and 2-MI (2-methylimidazole) were obtained from Aladdin (Shanghai, China) for ZIF-8 preparation. $MnSO_4 \cdot H_2O$ (>99%) and chlorin e6 (Ce6, ≥ 90%) were sourced from the same company. For buffer preparation, Na_2HPO_4 and KH_2PO_4 were obtained from Macklin (Shanghai, China). Folic acid PEG_{2k} amine (FA-PEG-NH_2, 97%, MW = 2000 Da) was also obtained from Macklin. $KMnO_4$ (>99.0%) was sourced from Sinopharm Chemical Reagent (Beijing, China). Hoechst 33342, DAPI and TUNEL were obtained from Beyotime Biotechnology (Shanghai, China). The Calcein-AM/PI kit (calcein acetoxymethyl ester/propidium iodide) was obtained from Beyotime for live/dead staining. An Annexin V-FITC/PI apoptosis kit was also obtained from Beyotime. Fetal bovine serum (FBS), RPMI-1640 medium and the 4T1 cell line were sourced from Pricella Biotechnology Co., Ltd (Wuhan, China). The same supplier was used for PBS (phosphate-buffered saline), trypsin-EDTA (0.25%), penicillin/streptomycin (P/S, 1%) and the cell counting kit-8 (CCK-8). DCFH-DA (2',7'-dichlorodihydrofluorescein diacetate, ≥ 97%) was obtained from Sigma-Aldrich (SL, USA) for intracellular ROS detection. Primary antibodies were obtained from Abcam (Cambridge, UK) for β-actin, Bax, Bcl-2 and cleaved Caspase-3. ROS probes were obtained from Thermo Fisher Scientific: DHR123 (dihydrorhodamine 123), SOSG (singlet oxygen sensor green) and HPF (hydroxyphenyl fluorescein).

Characterizations

ZPF and ZMPF morphology was examined with a Talos L120C G2 microscope (120 kV; Thermo Fisher Scientific, USA). Elemental composition was assessed by energy-dispersive spectroscopy (EDS) with a Talos F200X from the same manufacturer. For Fourier transform infrared (FTIR) measurements, a Nicolet iS50 spectrophotometer was used (Thermo Fisher Scientific, USA). Element concentrations were determined by ICP-OES with an Agilent 5110 (Agilent Technologies, USA). Diffraction patterns were obtained by X-ray diffraction (XRD) with the D8 ADVANCE instrument from Bruker AXS (Germany). The Zetasizer Nano ZSE instrument from Malvern Instruments (UK) was used for dynamic light scattering (DLS) measurements of hydrodynamic size. Absorbance measurements were made with a PE Lambda950 spectrophotometer (PerkinElmer, USA). Fluorescence measurements were made with an LS-55 spectrometer from the same manufacturer. Cellular fluorescence was examined by confocal laser scanning microscopy (CLSM) with the TCS SP8 STED 3X instrument from Leica (Germany). Flow cytometry (FCM) was performed using a CytoFLEX system (Beckman, USA). Magnetic resonance imaging (MRI) was performed on a 0.5 T MRI scanner (MiNiMR60, Niumag, China). Tissue section was performed using a Leica RM2016 slicer (Leica Biosystems, Germany). The UT-1001 ultrasonic therapeutic apparatus for sono-irradiation was purchased from Survow Technology (China). Routine blood analyses were measured by BC-2800vet Hematology Analyzer (Mindray, China).

The preparation of ZPF and ZMPF

ZIF-8 NPs were prepared by the reported synthesis [1]. Separate methanol solutions were prepared from $Zn(NO_3)_2 \cdot 6H_2O$ (8 mmol in 100 mL) and 2-methylimidazole (33.75 mmol in 100 mL). After mixing, the coordination reaction was conducted under stirring for 2 h at room temperature. The particles were isolated by centrifugation, followed by three methanol washes.

To prepare ZMPF, MnO_2 was deposited *in situ* onto ZIF-8 by an aqueous redox reaction between $MnSO_4$ and $KMnO_4$ [2]. A ZIF-8 dispersion (5 mL, 1 mg mL^{-1}) was supplemented dropwise with $KMnO_4$ solution (20 μL, 0.1 M). $MnSO_4H_2O$ solution (20 μL, 0.15 M) was then introduced. ZIF-8@MnO_2 NPs were obtained after continuous stirring for 15 min. Subsequently, folic acid PEG_{2k} amine (FA-PEG_{2k}-NH_2) were added into the mixture and stirred for 30 min, yielding crude ZMPF.

For comparison, ZPF was prepared using the same PEG-FA modification procedure, but without the MnO_2 deposition step. Specifically, FA-PEG2k-NH2 was added to the ZIF-8 dispersion (5 mL, 1 mg mL^{-1}). Crude ZPF was obtained after the mixture had been stirred for 30 min.

Afterward, the ZPF and ZMPF preparations were centrifuged for product collection. Each product was washed with DI water for three times.

Stability of ZMPF

ZMPF was dispersed in DI water at 200 μg mL^{-1}. Hydrodynamic size was measured by DLS after incubation for 0, 6, 12, 18 or 24 h.

***In vitro* ROS detection**

Sonodynamic properties of ZPF and ZMPF. Fluorescent probes DHR123, HPF and SOSG were used to detect $O_2^{\bullet-}$, •OH and $^1O_2$, respectively [3]. ZPF (MnO_2-free control) or ZMPF (MnO_2-decorated platform) was dispersed in PBS (pH 7.4) at 33 μg mL^{-1}. The selected probe was added at 10 μM. US exposure was applied with a 40% duty cycle and an intensity of 1.5 W cm^{-2}. The fluorescence was monitored every 1 min and normalized as F/F_0. The DHR123, HPF and SOSG signals were measured at 525 nm.

Chemodynamic and sonodynamic activities of ZPF and ZMPF were assessed at pH 7.4, 6.5 and 5.5, with or without H_2O_2 at 100 μM. ZPF or ZMPF was tested at 33 μg mL^{-1}. The probes were used separately at 10 μM. $O_2^{\bullet-}$ detection was performed with DHR123, •OH detection with HPF and $^1O_2$ detection with SOSG. US was applied with a duty cycle of 40% and an intensity of 1.5 W cm^{-2}. Readings were taken every 1 min at 525 nm. Fluorescence changes were normalized to the initial reading and expressed as F/F_0.

Cell experiments

RPMI-1640 was used for 4T1 culture, with FBS (10%) and P/S (1%) added. Incubation was performed at 37 ℃ under 5% CO_2. At 80%-90% confluence, cells were detached with trypsin, and then subcultured or seeded in cell plates for subsequent experiments. Cell irradiation was performed using a flat, unfocused transducer (UT-1001, Survow Technology, China). The transducer had no designed focal distance. Medical ultrasound coupling gel was applied between the transducer surface and the underside of the culture plate, as shown in Figure 4I. The ultrasound output was calibrated by the manufacturer. Cells were exposed for 3 min at 1.0 MHz and an intensity of 1.5 W cm^{-2}, with a 40% duty cycle.

Cytotoxicity assay

For the cytotoxicity assay, incubation was performed at 37 ℃ under humidified conditions (95% air, 5% CO_2). RPMI-1640 was used with FBS (10%) and streptomycin/penicillin (1%). Each well of a 96-well plate was inoculated with 5×10^3 cells and incubated for 24 h. ZPF or ZMPF was added at 0, 5, 10, 15, 20, 25, 30 or 50 μg mL^{-1}, respectively. Following the 4 h incubation, cells were treated with or without US irradiation. Exposure was applied for 3 min at 1.0 MHz and an intensity of 1.5 W cm^{-2}, with a 40% duty cycle. A further 20 h incubation was allowed before CCK-8

measurements. Each well containing 100 μL culture medium was supplemented with 10 μL CCK-8 reagent (Pricella Biotechnology Co., Ltd). Absorbance was measured at 450 nm with a ReadMax1900 plate reader after 2 h. Wells that received neither material treatment nor US irradiation served as the control group. Percentage viability was obtained by dividing the treated-well absorbance by the control-well absorbance and multiplying by 100%.

***In vitro* cellular uptake assay**

Confocal imaging. Confocal culture dishes were inoculated with 5×10^4 4T1 cells per dish, followed by overnight culture. ZMPF@Ce6 was then added at ZMPF and Ce6 concentrations of 20 and 0.5 μg mL^{-1}, respectively. Uptake was assessed after incubation for 0, 0.5, 2 or 4 h. After incubation, PBS washing was performed, and nuclei were labeled with Hoechst 33342. Live cells were imaged by CLSM with a TCS SP8 STED 3X instrument from Leica. Hoechst 33342 fluorescence was recorded at 420-470 nm using 405 nm excitation. The Ce6 signal was recorded at 660-700 nm with excitation set to 650 nm. Background correction and cellular fluorescence quantification were performed in ImageJ.

Flow cytometry. Uptake was assessed with Ce6-labeled ZMPF for confocal imaging and FITC-labeled ZMPF for flow cytometry. For the flow-cytometric assay, ZMPF and FITC concentrations were set to 20 and 0.5 μg mL^{-1}, respectively. Samples were prepared after incubation periods of 0, 0.5, 2 and 4 h. Following cell collection at each time point, free ZMPF@FITC was removed by thorough PBS washing. Internalization was quantified from the FITC signal measured by flow cytometry.

Live/dead assay [4]

For live/dead staining, 4T1 cultures were established for 24 h in confocal culture dishes, with 5×10^3 cells in each dish. Cells were treated for 4 h with either ZPF or ZMPF at 25 μg mL^{-1}. H_2O_2 was introduced into the medium at 100 μM before US exposure. Irradiation was applied for 3 min (1.0 MHz, 40% duty cycle, 1.5 W cm^{-2}). Groups with and without H_2O_2 were included for US alone, NPs alone and NPs+US. Cells without treatment were also included for comparison. Calcein-AM staining was used to identify live cells, and PI staining to identify dead cells. The stained cells were then examined by CLSM.

Evaluation of intracellular ROS generation

Intracellular ROS was assessed in 4T1 cells plated at 5×10^3 cells per dish in confocal culture dishes and incubated for 24 h. Nanoparticle treatment was applied for 4 h at 25 μg mL^{-1} (ZPF or ZMPF). DCFH-DA loading was then performed at 10 μM for 20 min. The medium was replaced with fresh RPMI-1640 before ultrasound exposure. Irradiation was applied for 0 or 3 min (1.0 MHz, 40% duty cycle, 1.5 W cm^{-2}). The oxidized DCFH-DA signal was imaged by CLSM at 520-540 nm with 488 nm excitation. Mean fluorescence intensity (MFI) was calculated in ImageJ for comparison of the treatment groups.

Apoptosis analysis by flow cytometry

For apoptosis analysis, 24-well plates were seeded with 3×10^5 4T1 cells per well. A 24 h culture period at 37 ℃ was allowed before treatment. The control, US, ZMPF and ZMPF+US groups were analyzed with the Annexin V-FITC detection kit by flow cytometry. A 4 h uptake period was allowed for cells treated with ZMPF. At this time, the US and ZMPF+US groups were irradiated simultaneously for 3 min (1.0 MHz, 40% duty cycle, 1.5 W cm^{-2}). All cultures were incubated for a further 4 h and collected at the same endpoint. After medium removal, the cells were detached

with trypsin and collected. After three PBS washes, Annexin V-FITC/PI staining was performed for 15 min at 25 ℃ in the dark. FCM measurements were obtained immediately after staining.

Western blot analysis

For western blot analysis, 4T1 cultures were established overnight in 24-well plates. Control, US, ZMPF and ZMPF+US groups were assigned, and the corresponding formulations were added. Ultrasound was applied for 3 min (1.0 MHz, 40% duty cycle, 1.5 W cm^{-2}). Cells were harvested after 12 h for total protein extraction. A BCA assay kit was used to determine protein concentrations before PAGE separation of the lysates. Bcl-2, Bax and Caspase-3 were probed with their respective primary antibodies. The membranes were then incubated with the appropriate secondary antibodies (horseradish peroxidase-conjugated).

Transcriptome sequencing and analysis [5]

For RNA sequencing, each well of a 6-well plate was seeded with 5×10^5 4T1 cells. After 24 h of culture, ZMPF was added to the combined-treatment group (ZMPF+US) at 25 μg mL^{-1}. A 6 h incubation was followed by US exposure for 3 min (1.0 MHz, 40% duty cycle, 1.5 W cm^{-2}). Cells in the control group received no treatment. RNA was isolated from each group with TRIzol and RNA concentrations were measured with a Nanodrop 2000 instrument (Thermo Fisher Scientific). Libraries were constructed according to the Illumina protocol (San Diego, CA). Briefly, random primers were used to synthesize the first cDNA strand. During synthesis of the second strand, dUTP was incorporated into the cDNA. End repair was performed on the double-stranded cDNA before A-tailing. Compatible Illumina adaptors were then ligated to the prepared ends. The final sequencing libraries were amplified by PCR and assessed with an Agilent 5300 bioanalyzer. Library quantification was performed by qPCR before sequencing with an Illumina NovaSeq X

plus instrument. RNA-seq services were obtained from Majorbio (Shanghai Majorbio Bio-pharm Biotechnology, Shanghai, China). Data processing was performed through the Majorbio Cloud Platform, and differential expression between the two groups was assessed with DESeq2.

Routine blood analysis

Healthy BALB/c mice were injected ZMPF intravenously at 10 mg kg^{-1}. At 48 h after dosing, red blood cells (RBCs) were collected by retro-orbital sampling for blood count analysis.

Hemolysis Assay [6]

Hemolysis was assessed using RBCs isolated from BALB/c mice by centrifugation at 3000 rpm and 4 ℃. To remove white cells, three washing steps were performed with 1×PBS. A 0.5 mL RBC suspension was combined with 0.5 mL ZMPF in PBS at each tested concentration. Positive and negative controls were prepared with water and PBS, respectively. After 4 h incubation at room temperature, each mixture was centrifuged for 10 min at 3000 rpm. The supernatant was collected for absorbance measurement with a plate reader (570 nm). For calculation, the sample absorbance was denoted A_{sample}, and the PBS control absorbance was denoted $A_{negative}$. The water control absorbance was denoted $A_{positive}$. Hemolysis (%) was calculated as $[(A_{sample} - A_{negative}) / (A_{positive} - A_{negative})] \times 100\%$.

***In vivo* MRI imaging and biodistribution**

In the 4T1 tumor model, ZPF or ZMPF was injected intravenously at 10 mg kg^{-1}. T_1-weighted images were acquired at 0, 1, 4, 8, 12 and 24 h with a 0.5 T MR scanner. Repetition time (TR) and echo time (TE) were set to 500 and 20 ms, respectively. Ten slices were acquired with a thickness of 2 mm, a gap of 0.5 mm and 4 averages. Tumor signal intensity was quantified in ImageJ from

the selected region of interest (ROI). For tissue distribution measurements, mice were euthanized 8 h after ZPF or ZMPF administration. The excised organs were fully dissolved in concentrated nitric acid. Zn and Mn concentrations in the resulting digests were determined by ICP-MS.

Animal experiments

BALB/c mice were purchased from GemPharmatech (Nanjing, China) at 5 weeks of age; only females were used. The mice were maintained in specific pathogen-free (SPF) animal rooms.

In vivo cancer therapy

The right flank was inoculated subcutaneously with 5×10^5 4T1 cells to establish tumors in female BALB/c mice aged 5 weeks. At a tumor volume of approximately 80 mm^3, mice were randomized to six groups (n = 5 per group). PBS alone was administered to the control group; the other groups were US, ZPF, ZMPF, ZPF+US and ZMPF+US. ZPF or ZMPF was injected intravenously on day 0, day 2 and day 4. The dose was 10 mg kg^{-1} per injection. For US treatment, tumors were irradiated 8 h after each injection for 5 min (1.0 MHz, 40% duty cycle, 1.5 W cm^{-2}). Tumor size and body weight were measured at 2-day intervals throughout the 14-day study. Volume was calculated from the tumor size as $width^2 \times length/2$. Tumors and major organs were collected after sacrifice at the study endpoint. Immunohistochemical staining was used to assess the therapeutic mechanism and biocompatibility.

Histopathological analysis

Tissues for H&E analysis were collected from each group after the mice had been sacrificed at the end of treatment. Tumor, kidney, lung, spleen, liver and heart samples were collected. Fixation was performed for 48 h with 4% PFA. The tissues were then dehydrated in 30% sucrose for 24 h.

The samples were embedded in optimal cutting temperature medium. Sections of 10 μm thickness were cut with a Leica RM2016 slicer. Ethanol washing was performed before hematoxylin staining (3 min) and eosin staining (1 min). After a PBS rinse, the stained sections were examined with a Nikon ci-s microscope.

Immunofluorescence analysis

Apoptosis in tumor sections were detected by TUNEL staining according to the instructions supplied by Beyotime. Tumors were fixed in 4% PFA before sectioning and TUNEL labeling. DAPI was used to label the nuclei in these sections. Images of the stained sections were recorded by CLSM.

In vivo generation of $O_2^{\bullet-}$ [7]

Mice bearing 4T1 breast tumors of approximately 100 mm^3 were given an intravenous injection of PBS, ZPF or ZMPF (100 μL). Both nanoparticle formulations were administered at 10 mg kg^{-1}. After 8 h, DHR123 (20 μL, 100 μM) was delivered intratumorally into each tumor. A 10 min interval was allowed before ultrasound treatment. Tumors were irradiated for 5 min (1.0 MHz, 40% duty cycle, 1.5 W cm^{-2}). The mice were then euthanized, and the tumors were excised. Samples were fixed in 4% paraformaldehyde (PFA) and cryosectioned. DAPI labeling was performed before fluorescence imaging of the tumor sections by CLSM.

Statistical Analysis

Statistical analysis was performed using GraphPad Prism 10.5.0. Group differences were assessed using Student's t-test, one-way ANOVA or two-way ANOVA. Data were presented as mean values or mean ±

standard deviation. Statistical significance was indicated as follows: ns, $P > 0.05$; *$P < 0.05$; **$P < 0.01$; ***$P < 0.001$; and ****$P < 0.0001$.

Supporting Figures and Tables

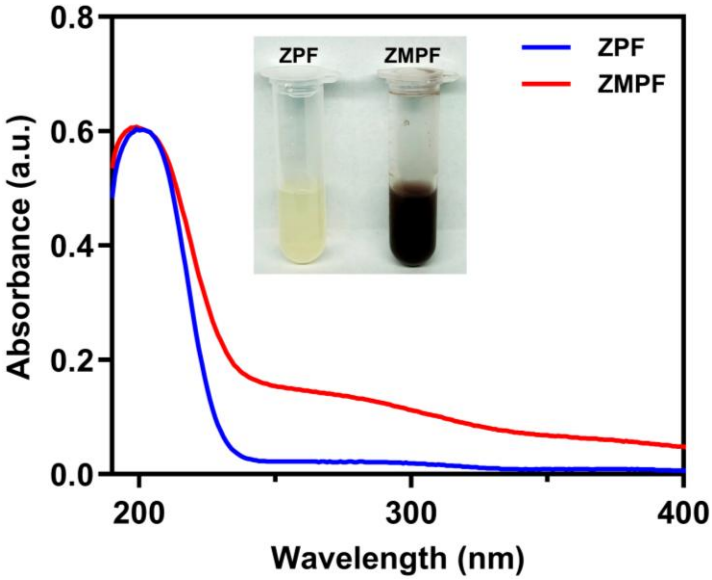


Figure S1. UV-vis absorption spectra of ZPF and ZMPF with the photograph of corresponding solutions as the inset.

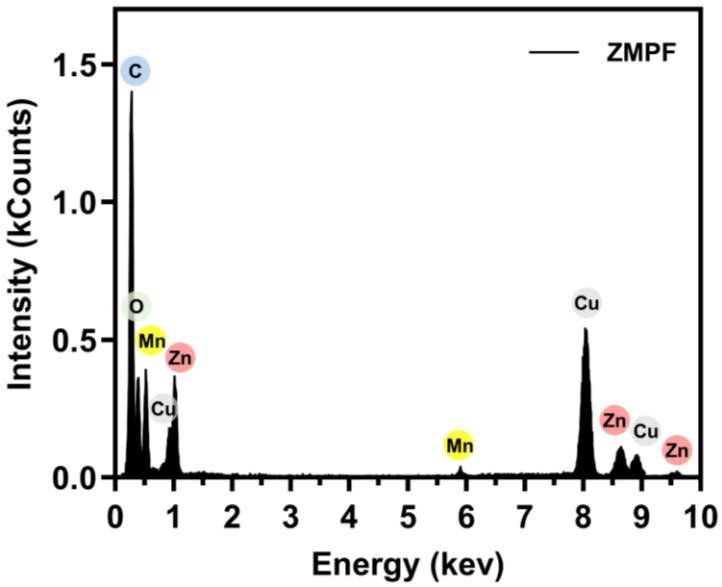


Figure S2. EDS spectrum of ZMPF.

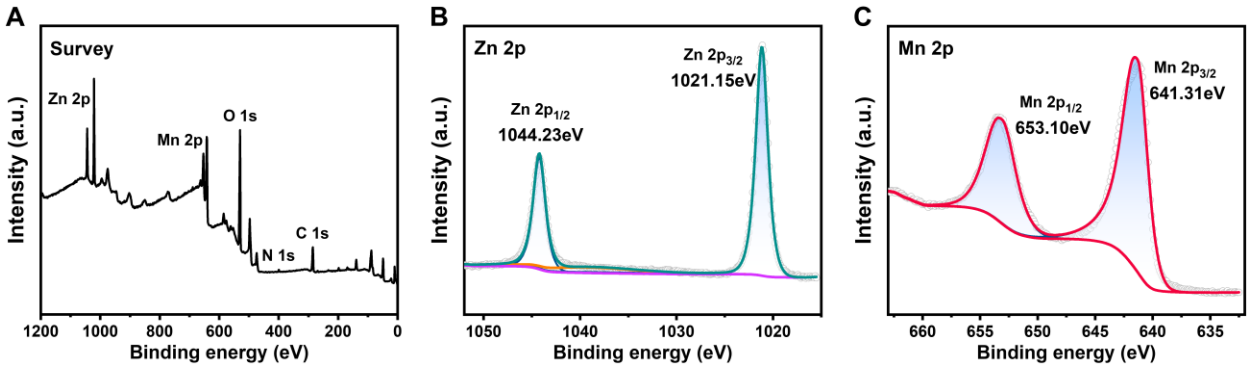


Figure S3. XPS results of ZMPF. (A) Survey spectrum. High-resolution XPS spectra of Zn 2p (B) and Mn 2p (C).

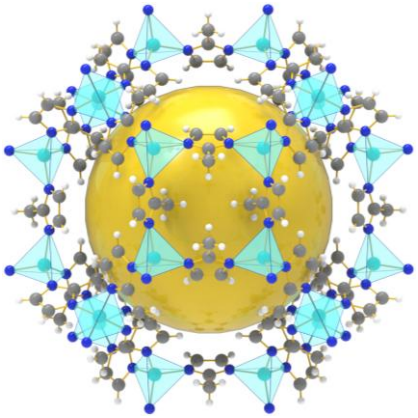


Figure S4. Schematic illustration of the ZIF-8 crystal structure.

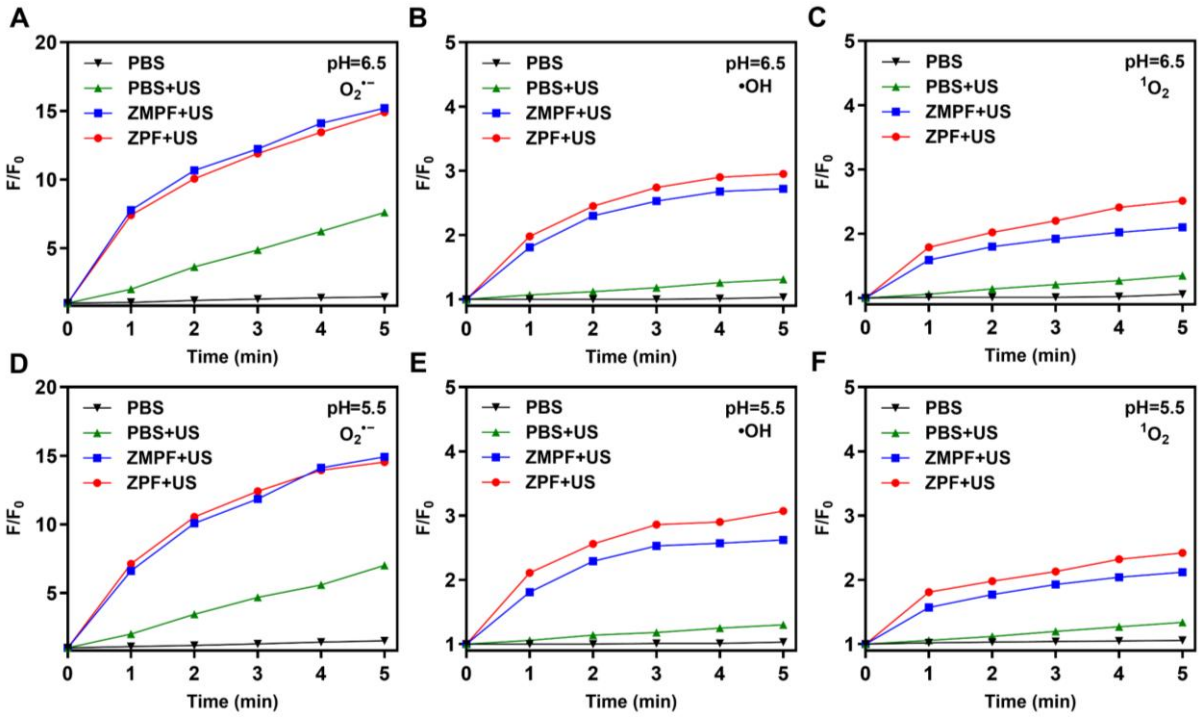


Figure S5. US-triggered ROS generation by ZPF and ZMPF at pH 6.5 and 5.5. ROS generation of $O_2^{\bullet-}$ (A, D), •OH (B, E) and $^1O_2$ (C, F) from ZPF+US, ZMPF+US, PBS+US and PBS in 10 mM PBS (pH = 6.5 and 5.5) at 37 ℃, respectively. F/F_0 represented the ratio of fluorescence signal of DHR123, HPF, SOSG before and after the US treatment (1.5 W cm^{-2}, 40% duty cycle) as a function of different treatment times, respectively, indicating the relative ROS generation efficiency.

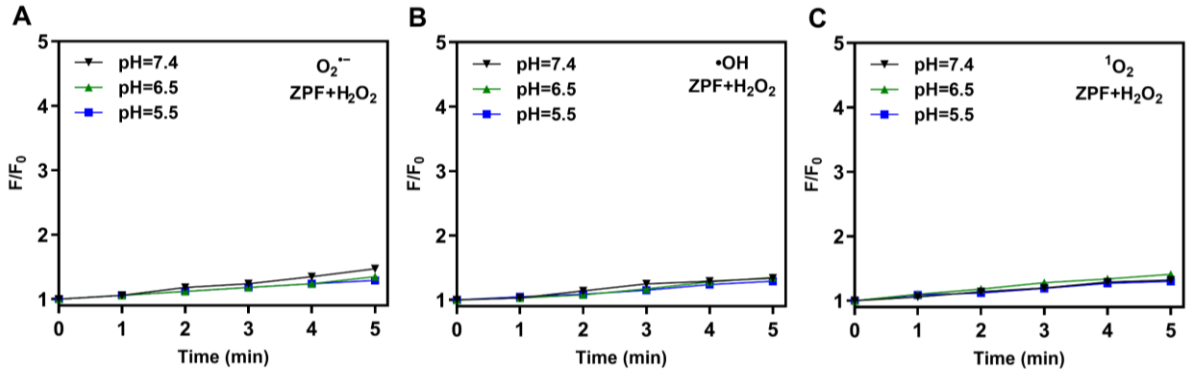


Figure S6. ROS generation by ZPF with H_2O_2 at pH 7.4, 6.5 and 5.5. ROS generation of $O_2^{\bullet-}$ (A), •OH (B) and $^1O_2$ (C) from ZPF+H_2O_2 in 10 mM PBS at 37 ℃, respectively. The fluorescence intensity at each time point (F) was divided by the initial intensity (F_0). Relative ROS generation was assessed using F/F_0.

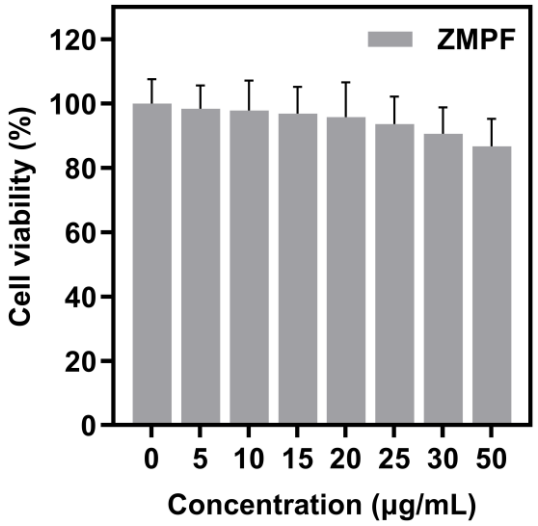


Figure S7. Viability of NIH/3T3 cells incubated with different concentrations of ZMPF (n = 6, mean ± s.d.).

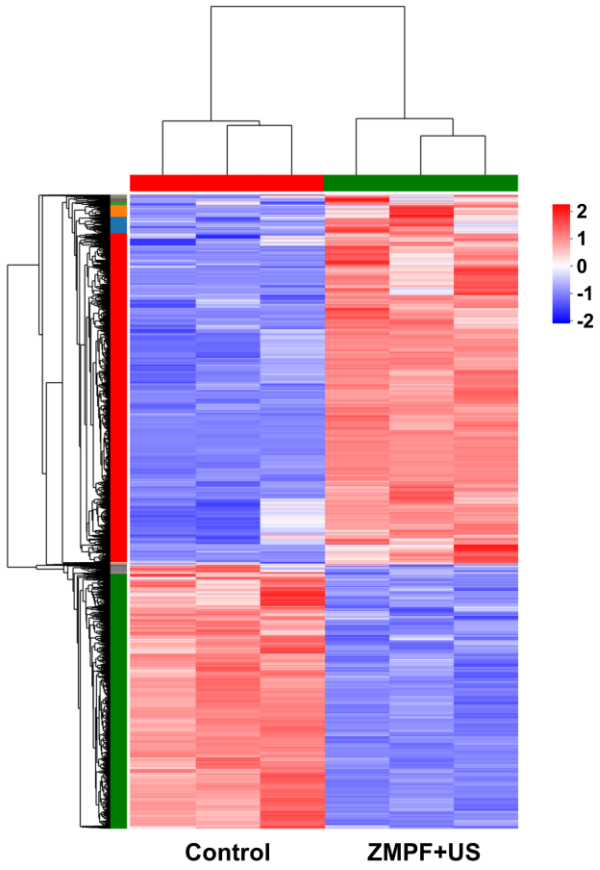


Figure S8. Heatmap of total DEGs in 4T1 cells between the control and ZMPF+US groups.

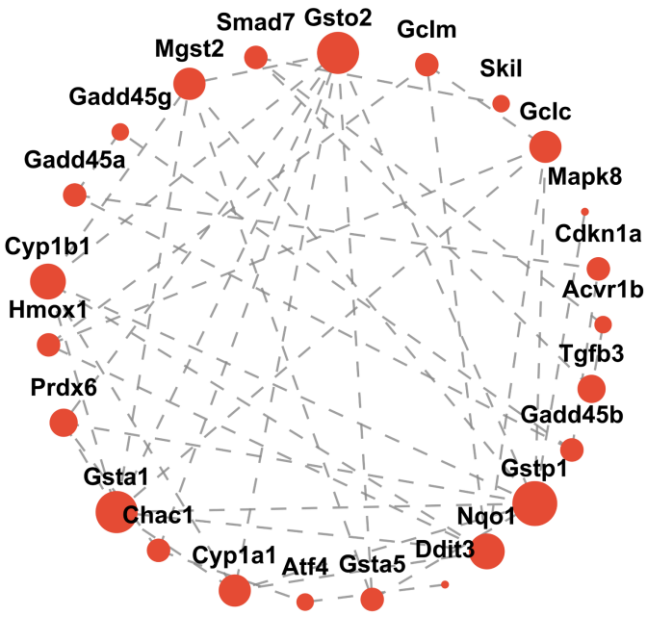


Figure S9. PPI network of the proteins encoded by DEGs.

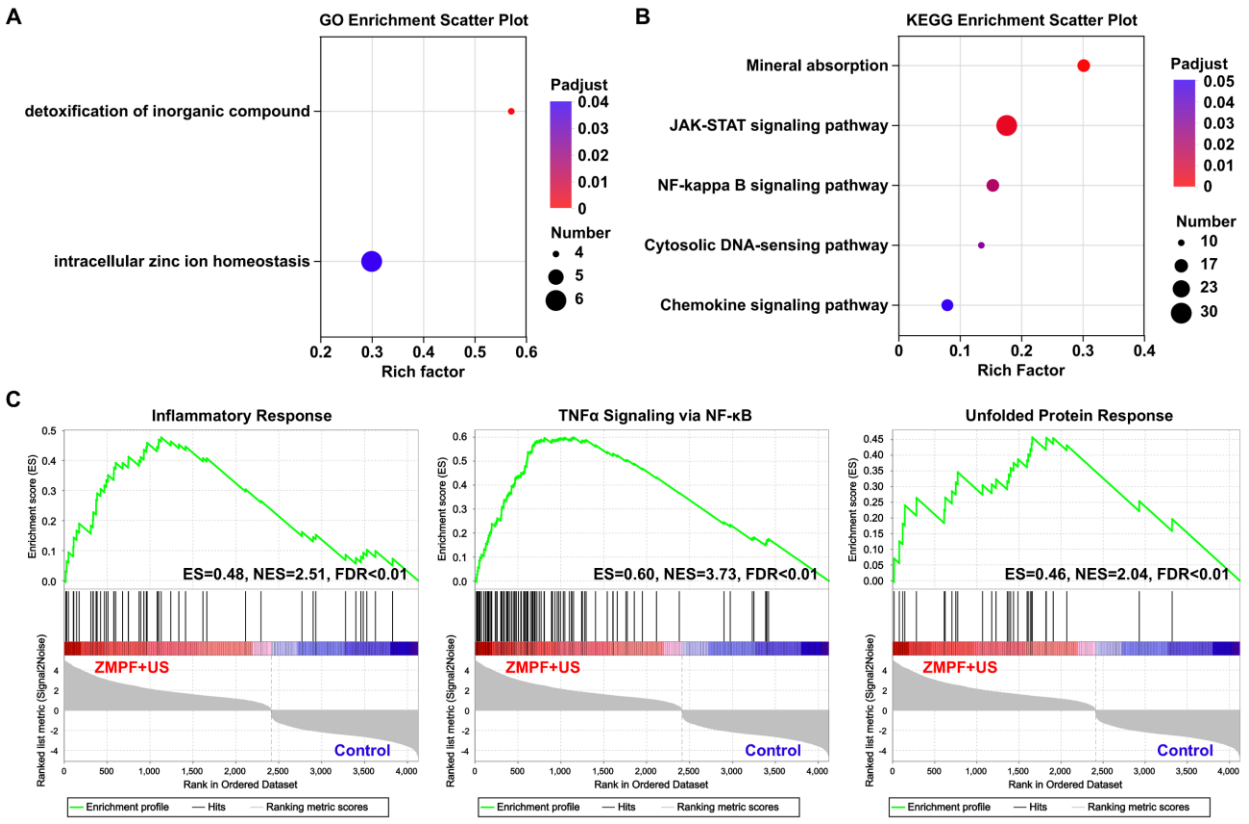


Figure S10. Metalloimmunological analysis of ZMPF+US-treated 4T1 cells by RNA sequencing. (A) GO enrichment of metal ion-related DEGs after ZMPF+US treatment. (B) Bubble diagram of the DEGs enriched in the immune- and metal-related KEGG pathway. (C) GSEA enrichment plots of hallmark inflammatory response, hallmark TNFα signaling via NF-κB and hallmark unfolded protein response gene set in the ZMPF+US treated as compared to the nontreated control.

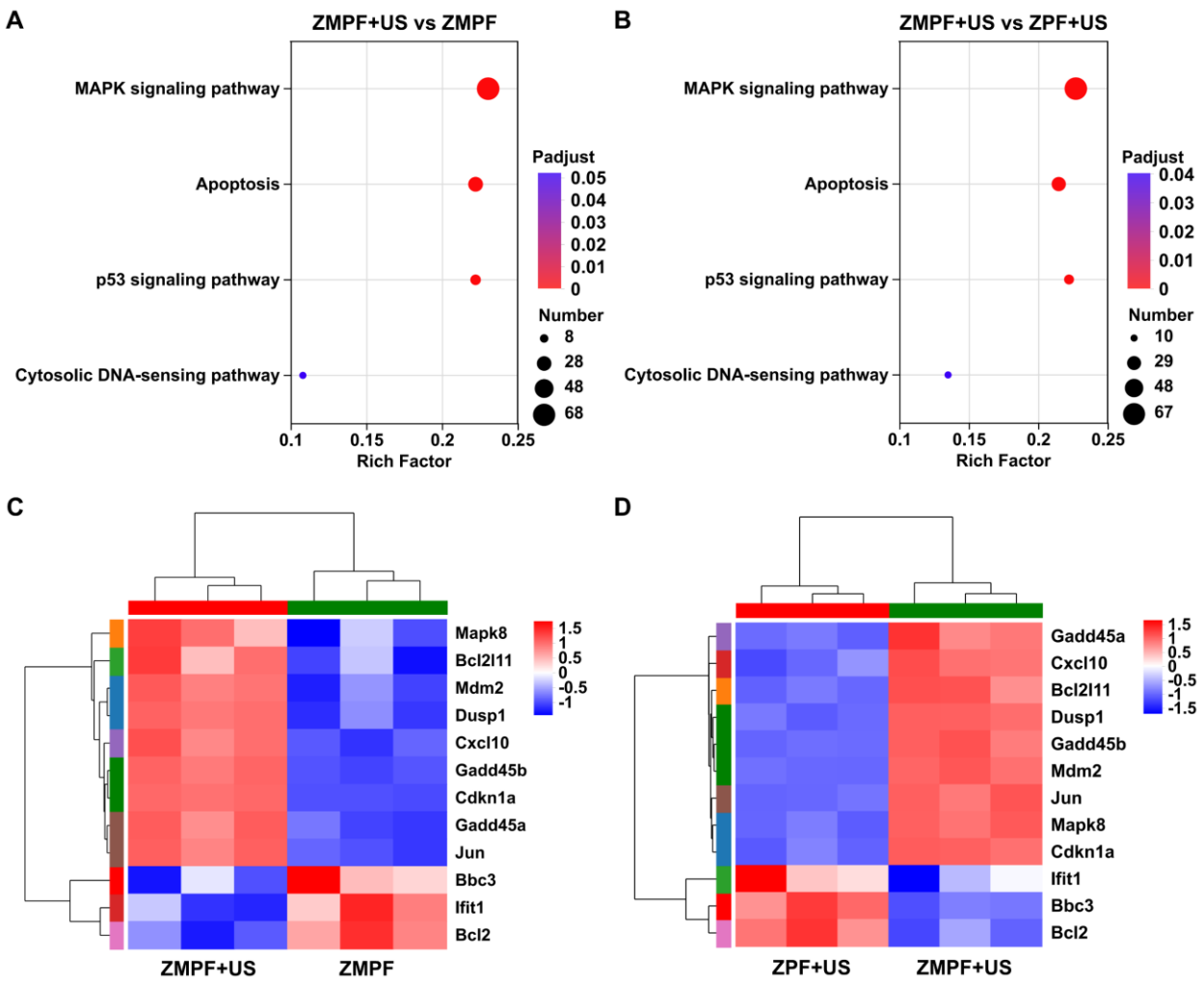


Figure S11. RNA sequencing analysis of 4T1 cells (ZMPF+US vs. ZMPF-treated group, ZMPF+US vs. ZPF+US-treated group). (A, B) Bubble diagram of the DEGs enriched in the KEGG pathway. (C, D) Heatmaps of DEGs related to apoptosis.

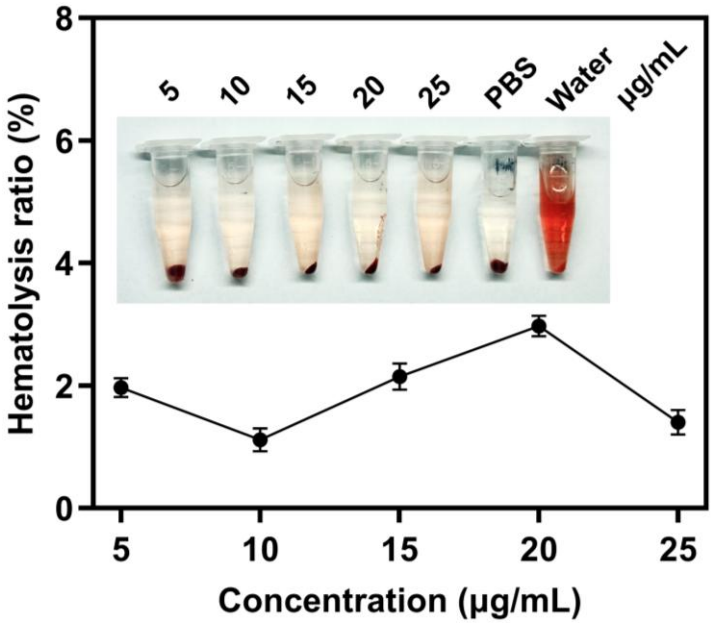


Figure S12. Hemolysis rates of red blood cells after adding ZMPF NPs at the indicated concentrations in PBS. Positive and negative controls were prepared with deionized water and PBS, respectively. The inset was the optical photograph. All data were presented as mean ± s.d. (n = 3).

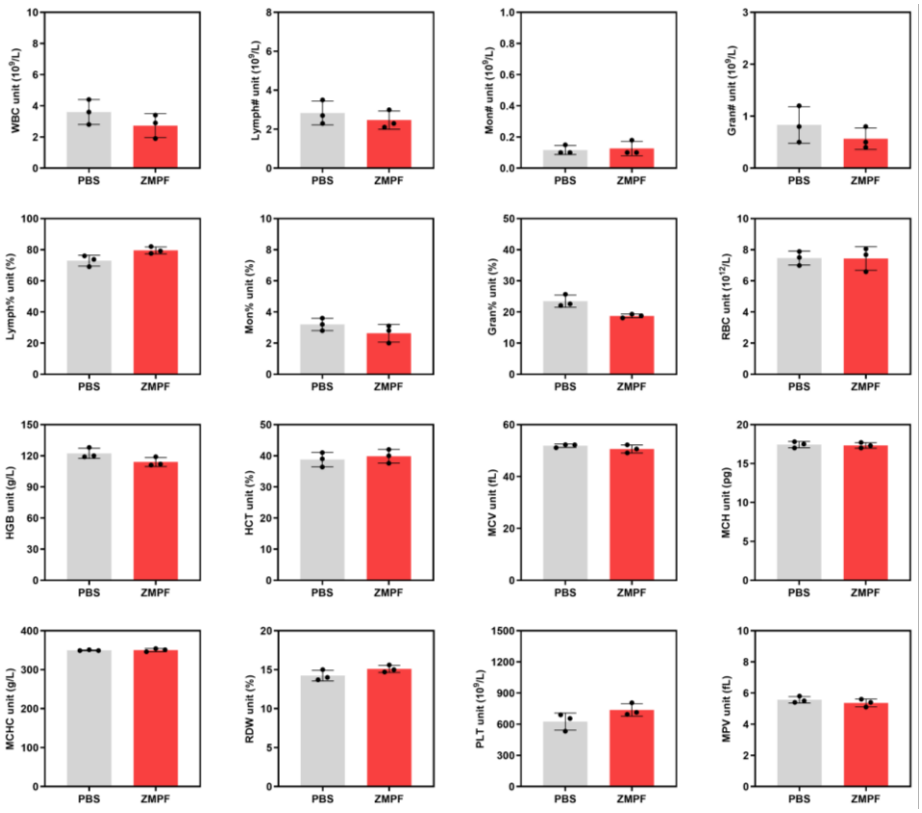


Figure S13. Routine blood analysis of normal BALB/c mice after intravenous injections with PBS and ZMPF (10 mg kg^{-1}) with an interval of 48 h for once, respectively (n = 3 independent mice). Data were shown as mean ± s.d.. WBC: white blood cells (normal range: 0.8-10.6); Lymph#: lymphocyte number (normal range: 0.6-8.9); Mon#: monocyte number (normal range: 0.04-1.4); Gran#: granulocyte number (normal range: 0.23-3.6); Lymph%: lymphocyte (%) (normal range: 40-92); Mon%: monocyte (%) (normal range: 0.9-18); Gran%: granulocyte (%) (normal range: 6.5-50); RBC: red blood cells (normal range: 6.5-11.5); HGB: hemoglobin (normal range: 110-165); HCT: hematocrit (normal range: 35-55); MCV: mean corpuscular volume (normal range: 41-55); MCH: mean corpuscular hemoglobin (normal range: 13-18); MCHC: mean corpuscular hemoglobin concentration (normal range: 300-360); RDW: red cell distribution width (normal range: 12-19); PLT: platelets (normal range: 400-1600); MPV: mean platelet volume (normal range: 4.0-6.2).

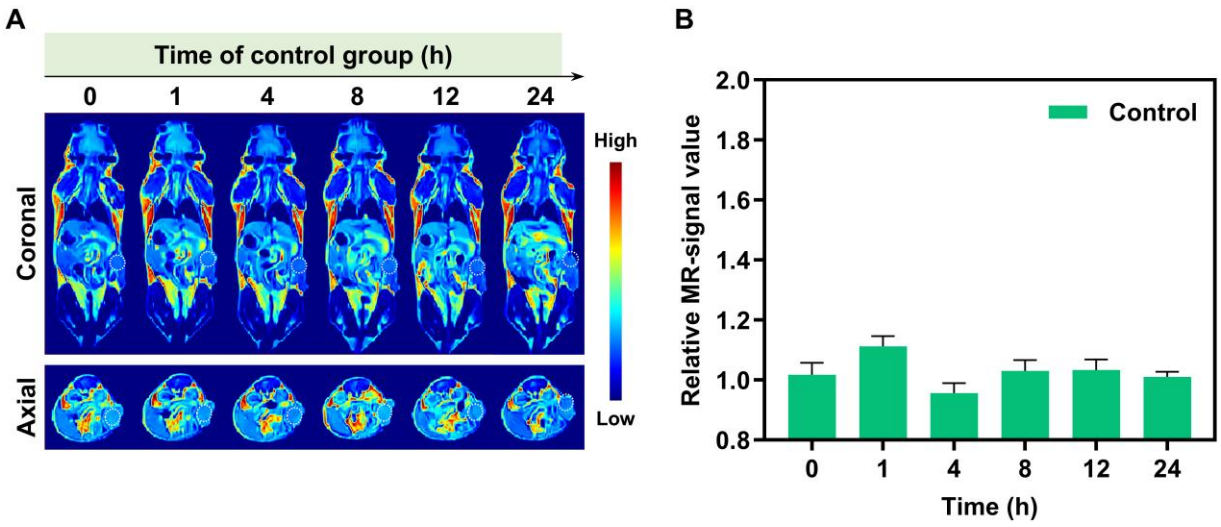


Figure S14. T_1-weighted MR imaging of untreated 4T1 tumor-bearing mice. (A) *In vivo* real-time T_1-weighted MR imaging of 4T1 tumor-bearing mice in control group at different treatment time. The white circles indicated the tumor region. (B) Quantification of T_1-MR signals from tumor in (A) (n = 3, mean ± s.d.).

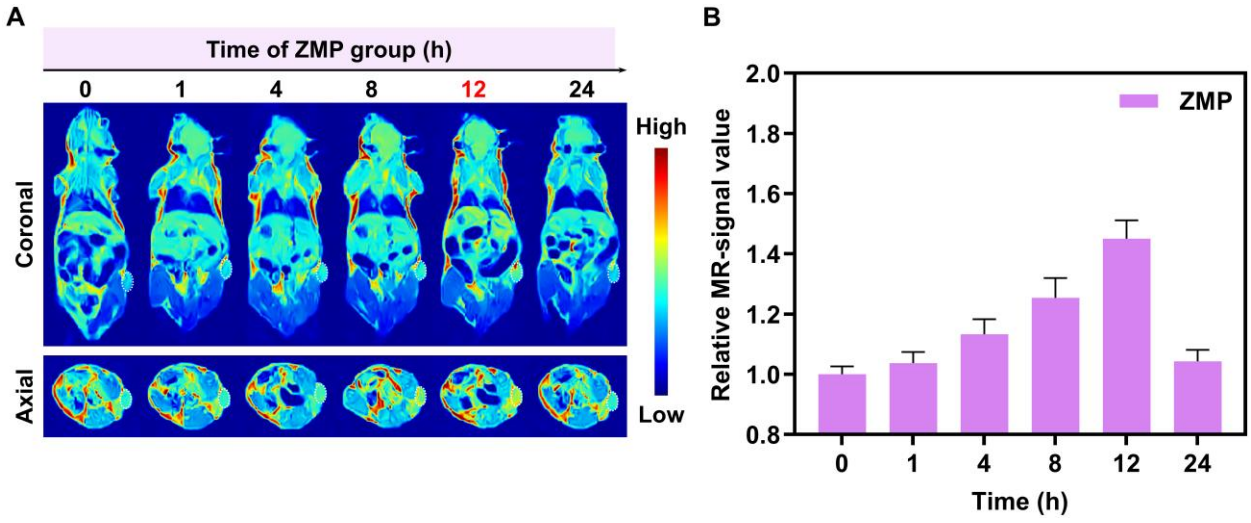


Figure S15. T_1-weighted MR imaging of non-targeted 4T1 tumor-bearing mice. (A) *In vivo* real-time T_1-weighted MR imaging of 4T1 tumor-bearing mice of ZMP group at different treatment time. The white circles indicated the tumor region. (B) Quantification of T_1-MR signals from tumor in (A) (n = 3, mean ± s.d.).

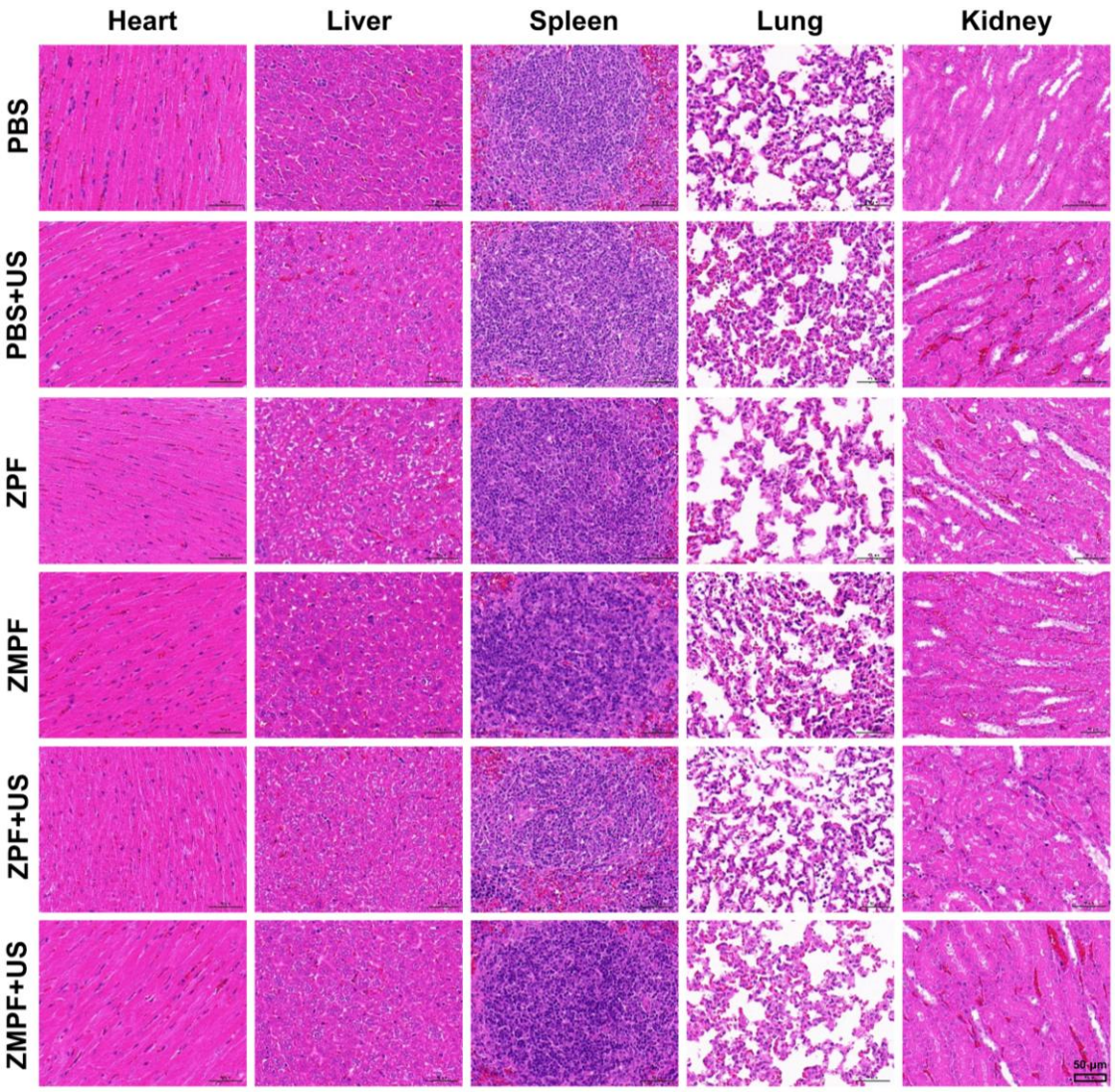


Figure S16. Histological analysis of the major organs. Samples were collected on day 14 from sacrificed BALB/c mice bearing subcutaneous 4T1 tumors. Kidney, lung, spleen, liver and heart sections were examined by H&E staining. Images were representative of three biologically independent mice. Scale bar = 50 μm.

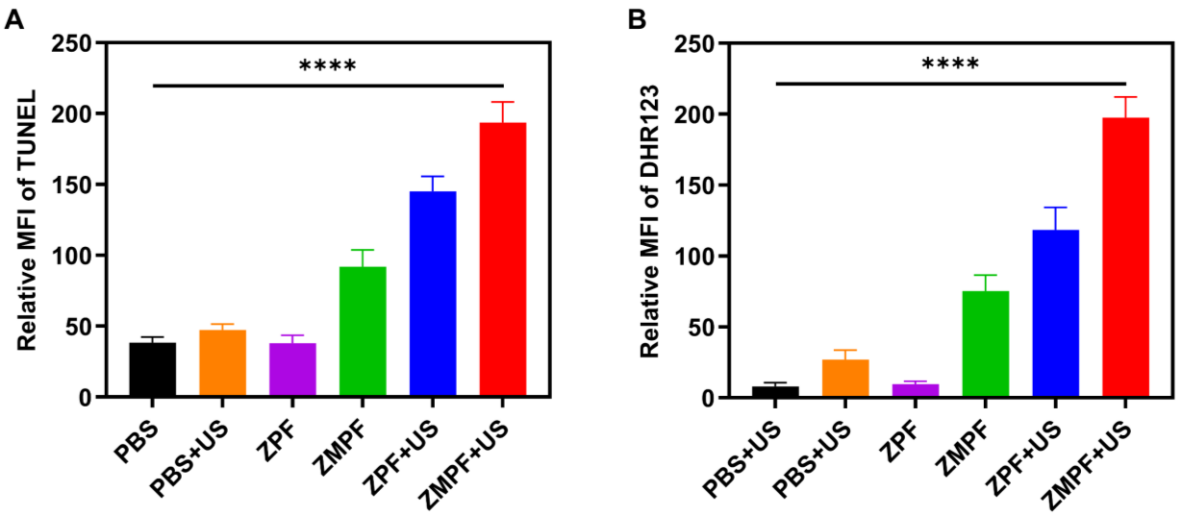


Figure S17. The corresponding fluorescence semi-quantitative results of TUNEL (A) and DHR123 (B) staining images. One-way ANOVA. ****$p < 0.0001$ ($n = 3$, mean ± s.d.).

Table S1. ICP-OES analysis of ZMPF sample.

Sample name	Results ICP-OES (mg L^{-1})	
	Zn	**Mn**
ZMPF	361.948	92.174

References

1. Wang W, Pan X, Yang H, Wang H, Wu Q, Zheng L, et al. Bioactive metal-organic frameworks with specific metal-nitrogen (M-N) active sites for efficient sonodynamic tumor therapy. ACS Nano. 2021; 15:20003-20012.

2. Zhang W, Li S, Liu X, Yang C, Hu N, Dou L, et al. Oxygen-generating MnO_2 nanodots-anchored versatile nanoplatform for combined chemo-photodynamic therapy in hypoxic cancer. Adv Funct Mater. 2018; 28: 1706375.

3. Huang J, Liu J, Wu J, Xu M, Lin Y, Pu K. Near-infrared chemiluminophore switches photodynamic processes via protein complexation for biomarker-activatable cancer therapy. Angew Chem Int Ed Engl. 2025; 137: e202421962.

4. Yao C, Xu Y, Tang J, Hu P, Qi H, Yang D. Dynamic assembly of DNA-ceria nanocomplex in living cells generates artificial peroxisome. Nat Commun. 2022; 13: 7739.

5. Zhang Z, Wu, H, Sathishkumar G, Mo F, Zhang K, Yu Y, et al. A multilayered responsive dressing for programmable exudate control and regenerative therapy of infected wounds. Adv Funct Mater. 2026; 36: e14784.

6. Zhang S, Sun Y, Zhang L, Zhang F, Gao W. Thermoresponsive polypeptide fused L-asparaginase with mitigated immunogenicity and enhanced efficacy in treating hematologic malignancies. Adv Sci. 2023; 10: 2300469.

7. Huang J, Su L, Xu C, Ge X, Zhang R, Song J, et al. Molecular radio afterglow probes for cancer radiodynamic theranostics. Nat Mater. 2023; 22: 1421-1429.